Dual Function Additives: A Small Molecule Crosslinker for Enhanced Efficiency and Stability in Organic Solar Cells

Joseph W. Rumer, Raja S. Ashraf, Nancy D. Eisenmenger, Zhenggang Huang, Iain Meager, Christian B. Nielsen, Bob C. Schroeder, Michael L. Chabinyc, and Iain McCulloch**

While organic electronic materials have potential as thin, lightweight, flexible, and crucially inexpensive devices,[1] they have often shown evidence of instability in chemical, photo, and thermal degradation.[2] Multijunction organic solar cells have exceeded 10% efficiency at research level,[3] but to be commercially useful it is regularly stated that they must have lifetimes in excess of 10 years, making device stability a primary concern.[4] A promising approach to addressing morphological instabilities of thin film bulk heterojunction devices involves photocrosslinking of the π-conjugated semiconducting donor polymer component, which allows the phase morphology to be 'locked' affording thermally stable blends, with suppressed fullerene acceptor crystallization (**Figure 1**).

Polymer-based solar cells are particularly attractive as they can be tailored to afford the required solubility and processability for high throughput printing in device fabrication, typically through the use of alkyl side-chains extending from the conducting polymer backbone,[5] while also being able to achieve optimal phase separation and tunable light absorption. High-performance devices are achieved in part by the optimization of device morphology to facilitate charge separation and transport, incorporating the π–π stacking of planar polymer backbones, the side-chain conformation, and miscibility of the fullerene acceptor molecules with the donor polymer.[6–9] However, such microstructures have a tendency for progressive phase separation on thermal ageing, with domains growing larger and therefore reducing excitonic charge separation as the effective interface area decreases. The presence of micron sized aggregates can also disrupt the film, leading to device shunting.

Crosslinking has been used in the literature to covalently bond polymer chains, "locking" the as-cast morphology and thereby conferring long-term thermal stability to devices.[10,11] Where this crosslinking occurs in the alkyl chain regions,[12] the conjugated polymer backbone is ideally unperturbed and device efficiency not just stabilized but also unimpaired.

Previously crosslinking strategies have largely focused on functionalizing a fraction of alkyl side-chain termini affixed to the polymer backbone with reactive groups. These functional groups have included halogens, vinyls, oxetanes, and azides, mainly exploiting radical, [2+2] cycloaddition and nitrene insertion reactions.[13] However, these approaches have significant drawbacks including: (1) the lengthy preparation of specifically functionalized polymers, (2) the addition or generation of potentially harmful species such as bromine radicals and photoacids, and (3) the typically low probability of two reactive groups occupying the required close proximity for reaction.

Recently, small molecule crosslinkers have attracted attention as they can be added to almost any polymer system, activated by UV (ultraviolet) light or thermal treatment.[14] Azides, for example, have been traditionally used in photoresists to produce nitrenes, inserting into C=C bonds in, for example, isoprene resin, emitting only inert nitrogen gas. More recently, sterically hindered fluorophenyl azides (sFPA's) have also been demonstrated to be directed to insert selectively into C–H bonds in the alkyl side-chains of a conjugated polymer backbone.[12,15,16] In addition, small molecule additives have also been previously demonstrated to boost the efficiency of organic solar cells, providing a more optimal microstructure, typically being alpha, omega-dihaloalkane or dithiol species.[17,18]

Here we simultaneously exploit both the small molecule crosslinker and additive concepts, through the preparation of an active bifunctional crosslinker which is structurally analogous to the α, ω alkane additives described earlier, utilizing the known bis-azide 1,6-diazidohexane (DAZH). This molecule was selected due to its facile synthesis from available starting materials, good shelf-life, and ease of characterization, arising from distinct infrared (IR) absorption peaks. The crosslinker is photoinitiated in an UV light curing process to avoid thermal degradation of the photoactive layer, and on activation, highly reactive nitrenes are formed from the azides, with inert nitrogen gas emitted as a side product.

DAZH was readily prepared in good yield and purity from the precursory dibromo alkane and sodium azide (**Figure 2**). The UV–vis absorption spectrum (dilute solution in chlorobenzene)

Dr. J. W. Rumer, Dr. R. S. Ashraf, Dr. Z. Huang, Dr. I. Meager, Dr. C. B. Nielsen, Dr. B. C. Schroeder, Prof. I. McCulloch
Department of Chemistry and Centre for Plastic Electronics
Imperial College London
London SW7 2AZ, UK
E-mail: jwrumer@imperial.ac.uk; i.mcculloch@imperial.ac.uk

Dr. N. D. Eisenmenger, Prof. M. L. Chabinyc
Materials Department
University of California Santa Barbara
Santa Barbara, CA 93106, USA

Prof. I. McCulloch
Physical Sciences and Engineering Division and SPERC
King Abdullah University of Science and Technology (KAUST)
Thuwal 23955–6900, Saudi Arabia

DOI: 10.1002/aenm.201401426

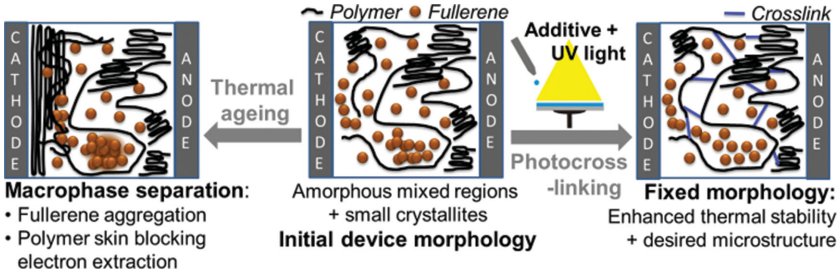

Figure 1. Crosslinking and thermal ageing: photocrosslinking should "lock" the as-cast morphology, conferring thermal stability, supressing formation of an electron-blocking polymer skin layer at the cathode, and fullerene crystals in the bulk.

shows no absorption above 400 nm, being significantly blue-shifted relative to typical organic semiconducting polymer absorption spectra maxima (Figure S1, Supporting Information). In the IR spectrum (**Figure 3**) the azide stretch was observable at ≈2100 cm^{-1}. After ≈1 month of storage in the dark at room temperature, the IR spectrum was repeated with no observable changes, indicating good shelf-life of the crosslinker. The thermal stability of the bis-azide was further investigated by thermogravimetric analysis (TGA) which showed thermal degradation to begin at ≈100 °C (see Figure S2, Supporting Information), allowing for room temperature processing.

To investigate the effect of crosslinking on thermal stability in organic solar cells, the polymer polysilaindacenodithiophene-benzothiadiazole (with *N*-octyl side-chains) and [6,6]-phenyl-C_{71}-butyric acid methyl ester (SiIDT-BT/PC[70]BM) were used, as together these materials can give a PCE of over 5% while being amorphous as-cast.[19] The UV exposure wavelength used for photocrosslinking is an inherent property of the functional group, being ≈254 nm for azides. The curing process was optimized as part of device fabrication (see below) to 10 min exposure at 254 nm (photocrosslinking) followed by 10 min thermal annealing at 70 °C (soft curing). The crosslinking reaction can be monitored by IR, with the azide stretch (≈2100 cm^{-1}) disappearing almost entirely from the blend on curing (Figure 3). Moreover, differential scanning calorimetry implies that a crosslinked network forms in the system: where the solid polymer and its drop-cast film (SiIDT-BT) exhibit a discernible melt at ≈350 °C, on addition of bis-azide DAZH and thin film curing, the melt is greatly suppressed, indicating encumbered movement in the system (see Figure S3, Supporting Information).

The UV–vis spectra of polymer thin films with and without crosslinker, both before and after curing, are largely the same, with the crosslinker only slightly enhancing aggregation and reducing the bandgap (**Figure 4**). This implies that crosslinking does not disrupt the polymer π-electron conjugation on an observable scale. This was further confirmed by gas chromatography–mass spectrometry (GC-MS) for a model system (see Figure S4, Supporting Information), where an equimolar mixture of bis-azide DAZH, aliphatic hexadecane and aromatic indenofluorene (a soluble, pure, small molecule analogue of the conjugated polymer backbone) and fullerene was irradiated and the products analysed. DAZH was no longer detected after curing and several new peaks emerged. Moreover, the aromatic peak increases in intensity relative to the aliphatic, indicating that DAZH reacts preferentially with the aliphatic species in such a thin film system, likely due to preferential partitioning in aliphatic regions of the film during the casting process. The mitigation of aromatic C=C addition and C–H insertion reactions by the carbene is important, as these could perturb the conjugation pathways, either by saturation of the bonds or, for the polymer, inducing steric hindrance and torsional twisting about the backbone. Such disruption could lead to reduced optical absorption and charge generation, accompanied by inhibition of charge transport. Additionally the addition of steric bulk may reduce ordering in the system, leading to reduced charge hopping between π-stacked polymers for example. Such reduced charge generation and transport would manifest as a reduced short-circuit current and power conversion efficiency in a photovoltaic cell. Additional gel permeation chromatography (GPC) experiments were performed to detect changes in the molecular weight of the fullerene on crosslinking (Figure S5, Supporting Information). Measurements were done by redissolving spin-coated films of fullerene with 10% bis-azide DAZH in hot chlorobenzene after curing, in which extra peaks emerge, attributable to the formation of higher molecular weight fullerene derivatives and oligomers, indicating that the fullerene may also react with DAZH in the curing process.

Bulk heterojunction thin film devices were prepared, using SiIDT-BT/PC[70]BM as the photoactive layer blend. Devices had a conventional architecture, prepared and studied under an inert atmosphere. As aforementioned, preliminary experiments revealed a need for soft-curing after UV exposure to mitigate electrode delamination: while no such thermal preannealing lead to rapid degradation, 10 min at 70 °C afforded device stability with minimally reduced initial performance. Hence a systematic study of UV exposure time, crosslinker functionality and amount was conducted, across an 85 °C inert atmosphere thermal ageing regime, an industry standard for realistic solar cell testing (Table S1, Supporting Information). For reproducibility, the quoted values are an average of at least 10 devices.[20]

The bis-azide DAZH exhibits a positive additive effect, yielding a substantial increase in as-cast device performance with the power conversion efficiency (PCE) increasing from 6.0% to 6.8% and 7.0%, for 5% and 10% wt DAZH (with respect to polymer), respectively (**Figure 5**). The increased as-cast PCE with DAZH present is due to an improved fill factor, which may result from a more optimal morphology yielding increased charge

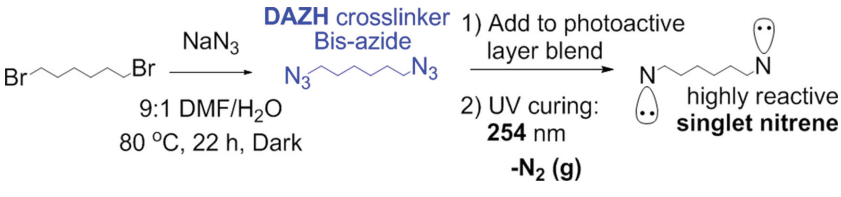

Figure 2. Synthesis of the bis-azide small molecule crosslinker 1,6-diazidohexane (DAZH).

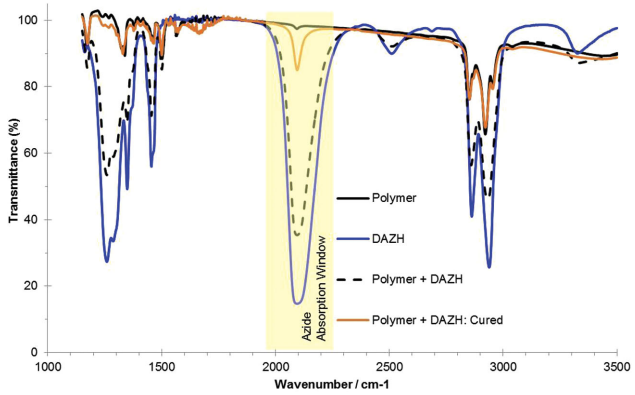

Figure 3. FTIR spectra of bis-azide DAZH and polymer (SiIDT-BT) and their blend before and after curing (thin films drop cast from dichloromethane on KBr plates).

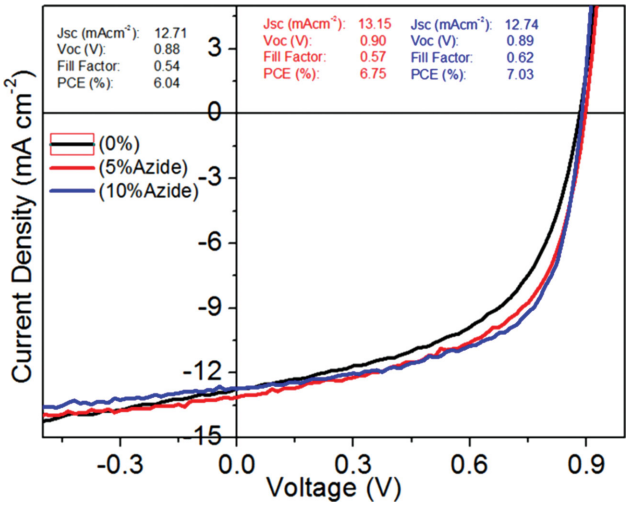

Figure 5. Current density–voltage curves for as-cast devices with varied amounts of DAZH bis-azide crosslinker present.

separation and improved transport. However, postcuring PCE decreases proportionally to UV exposure time, akin to the reference device.

The reference device exhibited a 6.0% as-cast PCE, dropping to 4% on exposure to 30 min 254 nm UV light. Overall this implies that the crosslinkers perturb the nanomorphology of intercalated transport pathways and/or conjugation pathways themselves (**Figure 6**), accompanied by photochemical instability of the system to shorter wavelength higher energy UV light.

Thermal stability of these devices was then tested by ageing at 85 °C under an inert atmosphere. After identical curing and ageing for 130 h, the devices containing bis-azide DAZH exhibited better stability, affording up to >80% retention of PCE (compared to <60% for the reference) (**Figure 7**). The highest PCE after ageing was found for devices with 10% DAZH, with 10 min UV exposure time (PCE of 4.1%, >70% retention of postcuring performance) (**Table 1**). The highest PCE after comparative ageing with 5% DAZH was 3.9%. Without additive, the device performance dropped to 3.5% PCE after ageing.

The mechanism of stability of bulk heterojunction organic photovoltaic devices is still under investigation, but morphology is known to play an important role, being highly sensitive to the exact properties of the constituent materials.[21,22] Recently, McGehee and co-workers showed that an initial drop in PCE can be due to formation of a thin electron blocking polymer skin underneath the cathode.[23] When ageing above the polymer's glass transition temperature (T_g), such movement of the polymer and fullerene species leads to a drop in V_{OC} and fill factor. In our case, a similar trend for the reference cell with a rapid drop in PCE was observed compared to cured devices containing bis-azide DAZH. It can be speculated that due to crosslinking, microstructure stability is achieved through not only frustration of fullerene aggregation, but also suppression of the diffusion that may lead to skin formation, possibly due to an increased T_g for the system,[24] thus providing the possibility of improved device stability and reduced degradation.

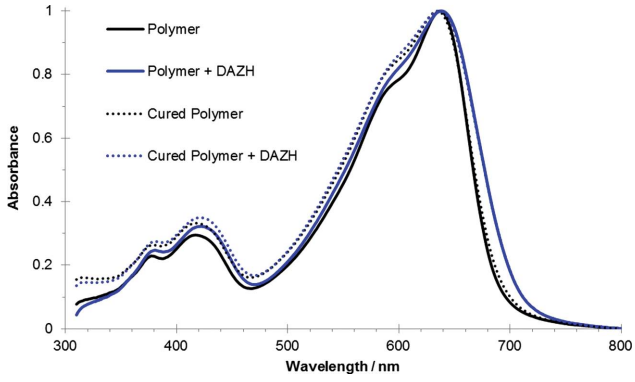

Figure 4. UV–vis spectra: polymer (SiIDT-BT) before and after UV curing, with and without bis-azide DAZH.

To better understand the initial efficiency changes and basis for thermal stability, the blend morphologies were investigated (**Figure 8**). Optical microscopy images of a series of as cast and aged thin film blends readily show the macroscale thermal stability conferred by photocrosslinking. Addition of bis-azide DAZH greatly suppresses fullerene crystallization, even with omission of the UV curing step, attributable to thermal activation of the crosslinker. This is shown by the lack of fullerene crystallization in these films as compared to the reference films. Furthermore, the bulk heterojunction microstructure has more of a fibrilar character as observed by atomic force microscopy (AFM). This is reflected in the positive additive effect observed for the DAZH-based devices, likely functioning in a similar way to the established additive 1,8-diiodooctane[17] and alkanedithiols,[16] improving ordering and packing of the polymer backbones.

Donor–acceptor phases of amorphous mixed and polymer rich are both discernible and expected to be beneficial for charge separation and transport.[25] The neat blend without crosslinker additives exhibits no such fibril formation and suffers from macroscopic fullerene crystallization. Comprehensive optical and AFM images may be found in the Supporting Information (Figures S6 and S7).

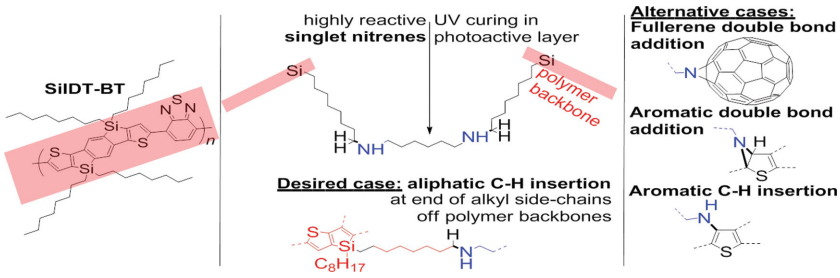

Figure 6. The photocrosslinking mechanism: singlet nitrenes react to form strong N–C covalent bonds, often by addition or insertion reactions, as illustrated for the SiIDT-BT polymer and a fullerene.

Notably the photocrosslinking reaction is carried out in the solid state at room temperature. This means cooperative movement is slow and the location in which the crosslinking reaction occurs will be the location that the crosslinker has been preferentially partitioned to during film formation from solution. The aliphatic spacer may promote its solubility, and likely partitioning in, the alkyl side-chain regions of the photoactive layer microstructure, a possible explanation for the fibril formation observed in DAZH-based devices. It is difficult to determine the exact location of the crosslinking, but it is also likely excluded from the highly ordered domains of the polymer and may partition into the disordered regions of the bulk heterojunction, conferring improved thermal stability without significantly impacting device performance.

As aforementioned, solvent additives such as diiodoctane (DIO) and alkane dithiols have been shown to greatly enhance device performance in a number of OPV blends.[17,26,27] Past studies have also shown that DIO increases the intermixing of fullerene derivatives with polymers and suggested that proximity of the polymer to pure fullerene aggregates is important for efficient charge separation and transport.[26,27] The DAZH acts not only as a stabilizing cross-linker but also as an additive in a similar mechanism to DIO and improves the OPV device performance due to an improved fullerene/polymer blend morphology. A simple solubility test confirmed the preferential solubility of PC[70]BM in DAZH (Figure S8, Supporting Information) in agreement with previous studies on other aliphatic solvent additives.[17,26,27]

In conclusion, we have utilized the small molecule crosslinker DAZH to confer thermal stability to bulk heterojunction organic photovoltaic devices which we speculate is as a result of frustrated fullerene aggregation and suppressed polymer skin formation at the cathode. This approach allows versatility, as the additive exhibits sufficient shelf-life and is readily activated by UV light in a scalable fashion, being solution processed and applicable to almost any spontaneously demixing blend system. Moreover, the DAZH additive affords an increase in as-cast device efficiency (from 6% to 7% in this case), thus being a dual function additive.

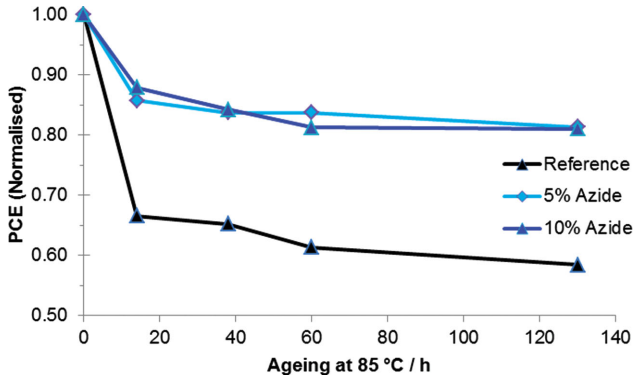

Figure 7. Photocrosslinking SiIDT-BT/PC[70]BM organic solar cells with bis-azide DAZH, with 30 min UV curing time: the bis-azide exhibits improved thermal stability after curing, compared to the as-cast reference with no crosslinker.

Experimental Section

General Experimental and Instrumental: NMR spectra were recorded on a Bruker DPX0 400 MHz spectrometer using an internal deuterium lock at ambient probe temperatures. Chemical shifts (δ) are quoted in ppm relative to TMS, with peak multiplicity (*t*, triplet; *m*, multiplet), integration, and coupling constants (*J*) quoted in Hz (uncorrected) as appropriate. $CDCl_3$ was used as the solvent for all spectra; the proton solvent residual peak is taken as: 7.26 ppm and the carbon solvent residual peaks as: 77.16 ppm. Infrared spectra were recorded using a solid state PKI Spectrum Two ATR or Perkin Elmer FTIR spectrometer. UV–vis detection was performed using an UV-1601 Shimadzu UV–vis spectrometer. Thermal gravimetric analysis (TGA) plots were obtained with a Perkin Elmer Pyris 1 TGA, heating under inert nitrogen gas at a rate of 5 °C min^{-1} in the range 30–800 °C. Differential scanning calorimetry (DSC) experiments were carried out on a TA Instruments DSC Tzero Q20 instrument, heating under inert nitrogen gas at a rate of 20 °C min^{-1} in the range –30 to –350 °C (3 cycles). The neat polymer was placed in the sample pan (2–4 mg); for the neat polymer thin film this was dissolved to solution in the pan using minimal chloroform which was then allowed to evaporate prior to measurement (thereby forming a thin film); in the case of the polymer and DAZH bis-azide crosslinker, the polymer was brought to solution using chloroform containing 10% wt DAZH with respect to the polymer sample mass, then on formation of the thin film cured in an identical fashion to the OPV cells. Gas chromatography-mass spectrometry (GCMS) analysis was performed by the Imperial College London Department of Chemistry Mass Spectrometry Service, using positive electrospray ionization; thin films were prepared by drop-casting on glass substrates (using a 1:1:1 molar ratio of compounds), curing in

Table 1. Device performance on fabrication and thermal ageing: organic photovoltaic cell power conversion efficiency (PCE) data for with and without the bis-azide **DAZH**.

DAZH[a]	UV exposure[b]	PCE (%): As-cast, after curing, after ageing					
		as-cast	cured	14 h	38 h	60 h	130 h
0%	–	6.0	–	3.9	3.9	3.6	3.5
5%	254 nm	6.8	5.4	4.4	4.1	3.8	3.7
10%	10 min	7.0	5.7	4.7	4.3	4.3	4.1

[a]Bis-azide crosslinker wt% added with respect to polymer. Devices had a conventional device architecture, see the Experimental Section for full details; [b]The UV exposure was followed by 10 min 70 °C thermal annealing (soft curing). Thermal ageing is at 85 °C under a nitrogen atmosphere, unencapsulated.

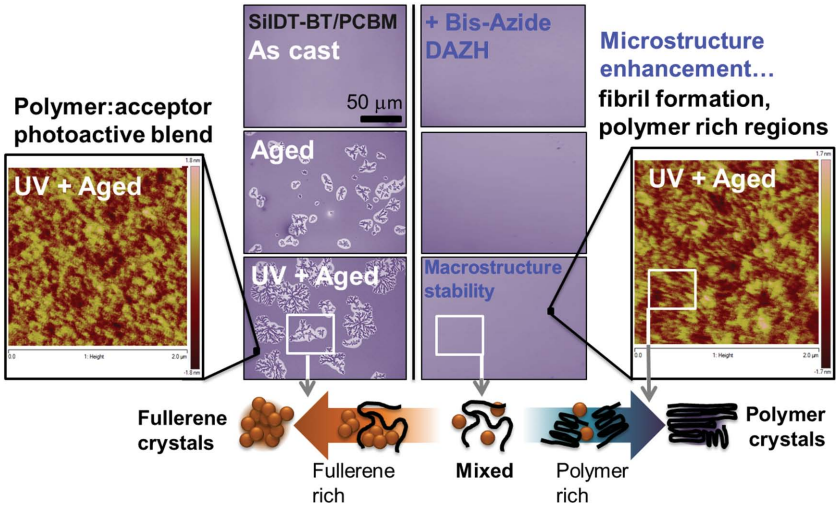

Figure 8. Crosslinking and thermal ageing morphology: small molecule additives confer macrostructure thermal stability, through suppressed fullerene crystallization (central optical microscopy images), with the bis-azide DAZH additionally enhancing the microstructure through fibril formation (flanking AFM images). Such a "double" picture of morphology highlights the various donor–acceptor phases in bulk heterojunctions and the microstructure basis of stability.

an identical fashion to OPV cells, and then redissolving in chloroform for analysis. Molecular weights: were recorded on an Agilent Technologies 1200 series gel permeation chromatography apparatus in chlorobenzene at 80 °C, using two PL mixed B columns in series, calibrated against narrow polydispersity polystyrene standards. Optical microscopy: images of blends with DAZH are taken directly from the solar cell substrates. Atomic force microscopy (AFM): was performed on an Agilent 5500 instrument in tapping mode directly on the solar cell substrates. Computational models were produced using density functional theory (DFT) in Gaussian 09 software at the B3LYP/6–31G* basis set theory level with hydrogens typically omitted in visualizing results.

Organic Photovoltaic Cell Device Fabrication: All organic photovoltaic devices have a conventional device architecture, glass/ITO/PEDOT:PSS/photoactive layer/Ca/Al. The precoated ITO glass substrates were cleaned with acetone and isopropyl alcohol under sonication, followed by drying and oxygen plasma treatment during seven minutes. A 30 nm layer of PEDOT:PSS was spin-coated onto the plasma-treated ITO substrate and baked at 150 °C for 20 min. The photoactive layer was spin-coated (preliminary: 2000 rpm; reoptimized: 1500 rpm) from a 1:3.5 blend of polymer:acceptor dissolved in *o*–dichlorobenzene. Photocrosslinking was performed using a low intensity hand-held (8 W) UV lamp, set to emit 254 nm light, the bulb positioned ≈1 cm from the substrates, followed by thermal curing (preliminary: 140 °C; reoptimized: 70 °C; both 10 min) in the glove box. The cathode was finally deposited by thermal evaporation under high vacuum (10^{-6} mbar) through a shadow mask. The pixel size, defined by the spatial overlap of the ITO anode and Ca/Al cathode, was 0.045 cm^2. The device characteristics were obtained using a xenon lamp at AM1.5 solar illumination (Oriel Instruments). Ageing was performed in the glove box (inert nitrogen atmosphere) at 85 °C in ambient light (devices not encapsulated).

Synthetic Procedures: Detailed experimental procedures are described below. All solvents, reagents and other chemicals were used as received from commercial sources at reagent or guaranteed reagent grade; all reactions were performed in the absence of light throughout (glassware wrapped in aluminum foil) using anhydrous chemicals under an argon atmosphere.

DAZH: Caution: Take Care When Handling Azides: To a solution of 1,6-dibromohexane (4.76 g, 19.5 mmol) in 9:1 (v/v) DMF/H_2O (total 100 mL) was added sodium azide (3.80 g, 58.5 mmol) and the mixture stirred under air at 80 °C for 16 h. The mixture was allowed to cool to room temperature, extracted with diethyl ether (3 × 50 mL), the combined organic extracts being dried over anhydrous magnesium sulphate, filtered and concentrated in vacuo to afford the title compound as a clear colorless oil (3.24 g, 99%). ^{1}H NMR (400 MHz, $CDCl_3$), δ (ppm): 1.35–1.49 (*m*, CH_2, 4H), 1.55–1.67 (*m*, CH_2, 4H), 3.28 (*t*, J = 6.8 Hz, N_3CH_2, 4H); ^{13}C NMR (400 MHz, $CDCl_3$), δ (ppm): 26.4, 28.8, 51.4; IR (KBr thin-film) 2940, 2862, 2100, 1454, 1350, 1260.

Supporting Information

Supporting Information is available from the Wiley Online Library or from the author.

Acknowledgements

The authors are very grateful to Prof. J. R. Durrant for useful discussions regarding organic photovoltaics and their stability and Dr. Lisa D. Haigh for mass spectrometry guidance and analysis, both of Imperial College London. This work was carried out with funding from Solvay, EC FP7 Project X10D; the Centre for Plastic Electronics at Imperial College London, Doctoral Training Centre (Grant Nos. EP/G037515/1 and EPSRC EP/I002936), NSF (Grant No. CHE 1026664), and the National Research Fund of Luxembourg. The authors declare no competing financial interest.

Received: August 15, 2014
Revised: December 17, 2014
Published online: February 11, 2015

[1] M. Pagliaro, G. Palmisano, R. Ciriminna, *Flexible Solar Cells*, Wiley-VCH, Weinheim, Germany **2008**.
[2] J. U. Lee, J. W. Jung, J. W. Jo, W. H. Jo, *J. Mater. Chem.* **2012**, *22*, 24265.
[3] J. You, L. Dou, K. Yoshimura, T. Kato, K. Ohya, T. Moriarty, K. Emery, C.-C. Chen, J. Gao, G. Li, Y. Yang, *Nat. Commun.* **2013**, *4*, 1446.
[4] T. D. Nielsen, C. Cruickshank, S. Foged, J. Thorsen, F. C. Krebs, *Sol. Energy Mater. Sol. Cells* **2010**, *94*, 1553.
[5] I. Meager, R. S. Ashraf, S. Rossbauer, H. Bronstein, J. E. Donaghey, J. Marshall, B. C. Schroeder, M. Heeney, T. D. Anthopoulos, I. Mcculloch, *Macromolecules* **2013**, *46*, 5961.
[6] D. Cheyns, K. Vasseur, C. Rolin, J. Genoe, J. Poortmans, P. Heremans, *Nanotechnology* **2008**, *19*, 424016.
[7] D.-H. Ko, J. R. Tumbleston, L. Zhang, S. Williams, J. M. DeSimone, R. Lopez, E. T. Samulski, *Nano Lett.* **2009**, *9*, 2742.
[8] S. A. Schmid, K. H. Yim, M. H. Chang, Z. Zheng, W. T. S. Huck, R. H. Friend, J. S. Kim, L. M. Herz, *Phys. Rev. B* **2008**, *77*, 115338.
[9] Z. Hu, B. Muls, L. Gence, D. A. Serban, J. Hofkens, S. Melinte, B. Nysten, S. Demoustier-Champagne, A. M. Jonas, *Nano Lett.* **2007**, *7*, 3639.
[10] B. J. Kim, Y. Miyamoto, B. Ma, J. M. J. Fréchet, *Adv. Funct. Mater.* **2009**, *19*, 2273.
[11] C.-Y. Nam, Y. Qin, Y. S. Park, H. Hlaing, X. Lu, B. M. Ocko, C. T. Black, R. B. Grubbs, *Macromolecules* **2012**, *45*, 2338.
[12] R.-Q. Png, P.-J. Chia, J.-C. Tang, B. Liu, S. Sivaramakrishnan, M. Zhou, S.-H. Khong, H. S. O. Chan, J. H. Burroughes, L.-L. Chua, R. H. Friend, P. K. H. Ho, *Nat. Mater.* **2010**, *9*, 152.

[13] J. E. Carlé, B. Andreasen, T. Tromholt, M. V. Madsen, K. Norrman, M. Jørgensen, F. C. Krebs, *J. Mater. Chem.* **2012**, *22*, 24417.
[14] L. Derue, O. Dautel, A. Tournebize, M. Drees, H. Pan, S. Berthumeyrie, B. Pavageau, E. Cloutet, S. Chambon, L. Hirsch, A. Rivaton, P. Hudhomme, A. Facchetti, C. Wantz, *Adv. Mater.* **2014**, *26*, 5831.
[15] B. Liu, R.-Q. Png, L.-H. Zhao, L.-L. Chua, R. H. Friend, P. K. H. Ho, *Nat. Commun.* **2012**, *3*, 1321.
[16] C. Tao, M. Aljada, P. E. Shaw, K. H. Lee, H. Cavaye, M. N. Balfour, R. J. Borthwick, M. James, P. L. Burn, I. R. Gentle, P. Meredith, *Adv. Energy Mater.* **2013**, *3*, 105.
[17] J. Peet, J. Y. Kim, N. E. Coates, W. L. Ma, D. Moses, aJ. Heeger , G. C. Bazan, *Nat. Mater.* **2007**, *6*, 497.
[18] H.-C. Liao, C.-S. Tsao, Y.-T. Shao, S.-Y. Chang, Y.-C. Huang, C.-M. Chuang, T.-H. Lin, C.-Y. Chen, C.-J. Su, U.-S. Jeng, Y.-F. Chen, W.-F. Su, *Energy Environ. Sci.* **2013**, *6*, 1938.
[19] R. S. Ashraf, Z. Chen, D. S. Leem, H. Bronstein, W. Zhang, B. Schroeder, Y. Geerts, J. Smith, S. Watkins, T. D. Anthopoulos, H. Sirringhaus, J. C. de Mello, M. Heeney, I. McCulloch, *Chem. Mater.* **2011**, *23*, 768.
[20] M. O. Reese, S. A. Gevorgyan, M. Jørgensen, E. Bundgaard, S. R. Kurtz, D. S. Ginley, D. C. Olson, M. T. Lloyd, P. Morvillo, E. A. Katz, A. Elschner, O. Haillant, T. R. Currier, V. Shrotriya, M. Hermenau, M. R. Riede, K. Kirov, G. Trimmel, T. Rath, O. Inganäs, F. Zhang, M. Andersson, K. Tvingstedt, M. Lira-Cantu, D. Laird, C. McGuiness, S. Gowrisanker, M. Pannone, M. Xiao, J. Hauch, R. Steim, D. M. DeLongchamp, R. Rösch, H. Hoppe, N. Espinosa, A. Urbina, G. Yaman-Uzunoglu, J.-B. Bonekamp, A. J. J. M. van Breemen, C. Girotto, E. Voroshazi, F. C. Krebs, *Sol. Energy Mater. Sol. Cells* **2011**, *95*, 1253.
[21] H. Wang, M. Shah, V. Ganesan, M. L. Chabinyc, Y.-L. Loo, *Adv. Energy Mater.* **2012**, *2*, 1447.
[22] H. Wang, M. Shah, C. Jaye, D. Fischer a.; V. Ganesan, M. L. Chabinyc, Y.-L. Loo, *Adv. Energy Mater.* **2013**, *3*, 1537.
[23] I. T. Sachs-Quintana, T. Heumüller, W. R. Mateker, D. E. Orozco, R. Cheacharoen, S. Sweetnam, C. J. Brabec, M. D. McGehee, *Adv. Funct. Mater.* **2014**, *24*, 3978.
[24] A. Hale, C. W. Macosko, H. E. Bair, *Macromolecules* **1991**, *24*, 2610.
[25] M. Pfannmöller, W. Kowalsky, R. R. Schröder, *Energy Environ. Sci.* **2013**, *6*, 2871.
[26] M. R. Hammond, R. J. Kline, A. A. Herzing, L. J. Richter, D. S. Germack, H-W. Ro, C. L. Soles, D. A. Fischer, T. Xu, L. Yu, M. F. Toney, D. M. DeLongchamp, *ACS Nano* **2011**, *5*, 8248.
[27] W. Chen, T. Xu, F. He, W. Wang, C. Wang, J. Strzalka, Y. Liu, J. Wen, D. J. Miller, J. Chen, K. Hong, L. Yu, S. B. Darling, *Nano Lett.* **2011**, *11*, 3707.